



## Strain-hardening and breakdown in poly(vinylidene fluoride) gels in methyl-ethyl-ketone and heptanone

Jessica Link, Mathieu Tauban, Riccardo Pieri, Olivier Sanseau, Paul Sotta

### ► To cite this version:

Jessica Link, Mathieu Tauban, Riccardo Pieri, Olivier Sanseau, Paul Sotta. Strain-hardening and breakdown in poly(vinylidene fluoride) gels in methyl-ethyl-ketone and heptanone. Journal of Polymer Science, In press, 10.1002/pol.20220156 . hal-03767660

**HAL Id: hal-03767660**

**<https://hal.science/hal-03767660>**


Submitted on 2 Sep 2022

**HAL** is a multi-disciplinary open access archive for the deposit and dissemination of scientific research documents, whether they are published or not. The documents may come from teaching and research institutions in France or abroad, or from public or private research centers.

L'archive ouverte pluridisciplinaire **HAL**, est destinée au dépôt et à la diffusion de documents scientifiques de niveau recherche, publiés ou non, émanant des établissements d'enseignement et de recherche français ou étrangers, des laboratoires publics ou privés.

## RESEARCH ARTICLE

# Strain-hardening and breakdown in poly(vinylidene fluoride) gels in methyl-ethyl-ketone and heptanone

Jessica Link<sup>1</sup> | Mathieu Tauban<sup>2</sup> | Riccardo Pieri<sup>3</sup> | Olivier Sanseau<sup>2</sup> | Paul Sotta<sup>1,4</sup> 

<sup>1</sup>Laboratoire Polymères et Matériaux Avancés, CNRS-Solvay, UMR 5268, Saint Fons Cedex, France

<sup>2</sup>Solvay R&I PM2D, Saint Fons Cedex, France

<sup>3</sup>Solvay Specialty Polymers, Bollate, Italy

<sup>4</sup>Univ Lyon, CNRS, UMR 5223, Ingénierie des Matériaux Polymères, Université Claude Bernard Lyon 1, INSA Lyon, Université Jean Monnet, Villeurbanne, France

## Correspondence

Paul Sotta, Ingénierie des Matériaux Polymères, CNRS UMR 5223, INSA Lyon, Villeurbanne Cedex F-69621, France.  
Email: [paul.sotta@insa-lyon.fr](mailto:paul.sotta@insa-lyon.fr)

## Abstract

Gelation kinetics and rheological properties of poly(vinylidene fluoride-co-hexafluoropropylene) [P(VDF-co-HFP)] solutions in methyl-ethyl-ketone and in 2-heptanone are investigated. Small-angle X-ray scattering measurements indicate that the systems undergo phase separation by a nucleation process. For concentrations between 6 and 10 wt% of copolymer, strain-hardening appears when gels are sheared in the nonlinear regime, around 50% of deformation. At some critical shear amplitude, the rheological response changes abruptly, but reversibly, from hyperelastic towards viscous liquid. This indicates that the system undergo fracture or shear banding, in bulk or at walls. In other words the continuous network formed by the elastic, polymer-rich phase is locally broken under high amplitude oscillatory shear, thus breaking down the overall elastic response of the material. More interestingly, when the strain amplitude is progressively decreased back to zero, the initial nonlinear viscoelastic behavior is quantitatively recovered. In addition, when the strain is removed, the solution turns back to gel state very fast as compared with thermal gelation kinetics. These observations indicate that the initial structure can heal within a short time. It is proposed that strain-hardening depends on the intrinsic hyperelastic behavior of the polymer-rich phase, which should have a high density of effective crosslinks and/or entanglements.

## KEYWORDS

gelation, LAOS, PVDF

## 1 | INTRODUCTION

In recent years, fluorinated polymers have attracted growing interest due to their versatility and their unique combination of properties.<sup>1–3</sup> Among this class of polymers, poly(vinylidene fluoride) (PVDF) and VDF-based copolymers

such as P(VDF-co-hexafluoropropylene) [P(VDF-co-HFP)] are emerging (co)polymers because of their high dielectric constant and their piezoelectric and pyroelectric properties.<sup>4–6</sup> Depending on the architecture of the copolymer, and specifically on the HFP comonomer molar fraction, these copolymers can be semicrystalline to amorphous and

This is an open access article under the terms of the [Creative Commons Attribution-NonCommercial-NoDerivs](https://creativecommons.org/licenses/by-nc-nd/4.0/) License, which permits use and distribution in any medium, provided the original work is properly cited, the use is non-commercial and no modifications or adaptations are made.

© 2022 The Authors. *Journal of Polymer Science* published by Wiley Periodicals LLC.

they can behave as thermoplastics or elastomers.<sup>1</sup> PVDF and related semicrystalline copolymers show a complex semicrystalline structure and a rich polymorphism. They are known to exist in up to five different crystal structures that have been widely studied by X-ray diffraction in the bulk state.<sup>7–9</sup> The predominant crystalline phase is the apolar  $\alpha$  polymorph (also denoted form II), generally obtained under melt crystallization. However, the polar  $\beta$  phase (or form I) attracts technological interest as it accounts for the piezoelectric and pyroelectric properties of the polymer.<sup>9,10</sup>

It has been found that PVDF and VDF-based copolymers form thermoreversible gels in certain solvents, the morphologies of which strongly depend on the exact nature of the solvent.<sup>11–17</sup> It is generally agreed that thermoreversible gelation is the result of the formation of a three-dimensional network in which the junction points consist in physical bonds.<sup>18,19</sup> Depending on the studied system, these physical bonds may result from hydrogen bonds, crystalline zones or liquid–liquid phase separation.<sup>20</sup>

Physical gels can be compared with chemically cross-linked systems, except that the junction points of the network are not chemical bonds.<sup>18</sup> The gelation process has been widely investigated on PVC, polyvinyl alcohol or acrylonitrile-vinyl acetate gels.<sup>21</sup> However, the nature of the junction points in the network has often been a subject of controversy. Indeed the nature and structure of these physical junction points are complex and depend on the considered system, so that they need to be further clarified. Crystallization and phase-separation appear to be the most recognized gelation mechanisms in polymer solutions. Paul suggested that gelation may be due to phase separation into polymer-rich and polymer-poor regions.<sup>20</sup> A classical model considers that gelation may occur due to hydrogen-bonding association of polymer chains.<sup>22</sup> Junction points may be small polymer crystallites interconnected by long chains. This last hypothesis was supported by thermodynamics of gel melting and crystallographic studies on the crystallites. As the crystalline regions are supposed to be small and constituted from only a small fraction of the total polymer, it seems difficult to clearly identify the rigid zones to crystallites in an unambiguous way.<sup>20</sup>

The gelation by crystallization mechanisms has been widely reported in the literature and may occur with highly crystallizable polymers such as polyethylene as well as with PVDF.<sup>11</sup> This mechanism depends on the experimental conditions. For example in the case of PVDF gels, the solvent nature influences the morphology of the polymer network. PVDF–acetophenone gels have been reported to have a spheroidal morphology while PVDF–glyceryl tributyrate gels would have fibrillar morphology.<sup>14,15</sup> Moreover, by changing the solvent, different

conformations of the crystallites can be obtained:  $\alpha$ -type crystals are obtained in PVDF–cyclohexanone gels and  $\beta$ -type crystals in PVDF– $\gamma$ -butyrolactone gels. Temperature also influences the morphology of the gels.

In addition to gelation through the formation of crystallites or hydrogen-bonding interactions, a third mechanism associated to liquid–liquid phase separation (or spinodal decomposition) was proposed by some authors.<sup>20,23,24</sup> They suggested that gelation is induced by separation of the system into polymer-rich and polymer-poor phases. Gels do not have a definite supramolecular structure and their structure depends on the gelation process. Studies on polyacrylonitrile (PAN), polyvinylalcohol (PVA), and gelatin solutions show that the mechanism of gelation through molecular aggregation or crystallization is not consistent in some cases. X-ray diffraction on PAN, PVA, and gelatin solutions and gels show that gelation occurs without change in light or X-ray scattering: thus, this gelation does not come from crystallization of hydrogen-bonds. Due to the optical heterogeneities of these samples, it was suggested that gelation could also occur via liquid–liquid phase separation. A molecular mechanism was therefore proposed. As the polymer solution is thermodynamically unstable at the gelation temperature, compact aggregates are formed and then connect to form a heterogeneous gel system.<sup>23</sup>

Gelation of polymer solutions involves a connectivity phase transition which causes the viscosity to diverge at the gel point. Since binary phase separation is driven by a diffusive process it is very likely that the onset of gelation would drastically slow down the kinetics of the phase separation process.

Liquid–liquid phase separation can sometimes occur in addition to or concomitantly with liquid–solid transition (crystallization), and the gelation mechanisms become more complex. This mechanism was investigated on PVDF gels in  $\gamma$ -butyrolactone by Cho et al.<sup>25</sup> They proposed that gelation in this solvent is a two-step process involving liquid–liquid phase separation followed by crystallization, though liquid–liquid phase separation alone may be responsible for gelation. Indeed, by performing DSC, SEM, and X-ray diffraction measurements on (dried) gels, they showed that, depending on the polymer concentration, different crystalline forms exist in the gel: form I for high concentrations of PVDF and forms I and II for low concentrations of polymer. They indicate that the gelation mechanism at high polymer concentration is due to the formation of crystalline zones. Conversely, at low concentrations, the solutions turn to gels in two steps with, first, liquid–liquid phase separation, followed by crystallization. Gelation may thus be caused only by the formation of polymer-rich zones and the overlapping of polymer chains in this phase, and crystallization may not be necessary to form a gel in that case.

Gelation of semicrystalline polymers is thus a complex phenomenon. The nature of the gel depends on the chain structure and molecular weight of the polymer, and also on the nature of the solvent.

The accepted definition of a gel is usually based on a rheological approach, defining a gel as a network which possesses an elastic modulus in oscillatory measurements extrapolated to zero frequency or at infinite time in relaxation experiments. The gel point may also be defined as the crossover of the shear storage ( $G'$ ) and loss ( $G''$ ) moduli in small-angle oscillatory shear measurements during a crosslinking reaction.<sup>26</sup> Another condition to define the gel state is the independence of the loss factor  $\tan\delta$  with the frequency.<sup>27</sup> These three methods are widely used to characterize the gelation time of polymer solutions. In addition numerous structural, thermal, mechanical analyses were performed on gels.

For PVDF in  $\gamma$ -butyrolactone, liquid–liquid phase separation has been considered as the cause of the gelation.<sup>25,28–30</sup> Investigations of PVDF gels formed in other solvents (aromatic diesters, acetophenone, ethyl benzoate, glyceryl tributyrate) have shown that crystallization may be responsible for the PVDF gelation.<sup>13,15,16,31</sup> These studies have also highlighted that the morphology of the PVDF gels strongly depends on the nature of the solvent.<sup>14</sup> Ohkura et al. expressed the gelation rate, defined as the inverse of the gelation time  $t_{\text{gel}}$  measured by a tube tilting method, as the product of a concentration-dependent factor  $f(C)$  and a temperature-dependent factor  $g(T)$ .<sup>32</sup>

The relationship between gelation and phase separation was studied.<sup>33,34</sup> Specifically, the respective roles of phase separation and crystallization were discussed. The differences observed depending on whether phase separation occurs in the nucleation or spinodal decomposition regimes were also discussed. Thus, the gelation of semicrystalline polymers is a complex phenomenon and the nature of the gel depends on the polymer chain structure and molecular weight as well as on the nature of the solvent, or more precisely on polymer–solvent interactions.

Kinetic studies of the gelation process have been performed in methyl-ethyl-ketone (MEK) and in others solvents to understand the gelation mechanism both from a macroscopic and a microscopic point of view.<sup>13–15,35</sup>

However, the structure, morphology and thermal behavior of these gels have mostly been studied in the dried state, considering that the morphology of the dried material is representative of the structure of the gel in the presence of solvent.<sup>14–16</sup>

In this article, we combine structural and dynamical investigation in order to elucidate the respective impacts of temperature and of large amplitude shearing on the structure and dynamical response of thermoreversible

gels of a P(VDF-*co*-HFP) copolymer in MEK and in 2-heptanone. Indeed, there may be a specific interest in studying PVDF solutions in such a solvent as heptanone, which has a high boiling temperature. In a previous work, the kinetics of gelation was investigated by tube tilting and rheology, while a combination of small-angle and wide-angle X-ray scattering (SAXS and WAXS) experiments were performed on the gels in the presence of solvent to probe the gelation mechanism and the structure of these systems.<sup>36</sup> In this article, we first show that gelation corresponds to the appearance of a nanometer structure. Some features of this structure are discussed in a semiquantitative way, based on SAXS. However, the emphasis is put here on the study of the response to these gels to large amplitude strain, which has not been reported yet. We analyze the nonlinear response of the gels to large amplitude oscillatory shear (LAOS) in details. We show that the gels exhibit self-healing behavior after breaking. Such dynamical mechanical experiments give pieces of information which are complementary to structural investigations.

## 2 | EXPERIMENTS

### 2.1 | Samples

The poly(VDF-*co*-HFP) copolymer considered in this work (Figure 1) was provided by Solvay (Solef® 21510). It is a linear random copolymer of vinylidene fluoride (VDF) and hexafluoropropylene (HFP) with a molar content of HFP below 20% and a molar mass in the range  $M_n \approx 150$ – $160$  kg/mol and  $M_w \approx 290$ – $300$  kg/mol. MEK has a boiling point temperature of 79 °C under 1 atm pressure. 2-heptanone (Sigma Aldrich, France) has a boiling point at 150 °C under 1 atm pressure. Both solvents were bought from Sigma Aldrich (France) and were used as received. Solutions of P(VDF-*co*-HFP) at different concentrations were prepared by dissolving appropriate amounts of the copolymer in the solvent at 80 °C and stirring with a magnetic bar at 500 rpm for 2 h in order to obtain homogeneous solutions. All solution preparations in MEK were performed under reflux to prevent solvent evaporation. The weight fraction of copolymer in

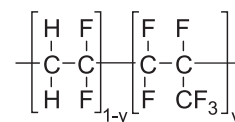


**FIGURE 1** Chemical structure of P(VDF-*co*-HFP).  $Y$  stands below 20 mol%. Note that VDF and HFP comonomers are randomly distributed along the chain

the solutions will be denoted  $\Phi_P$ . The solutions were cooled down to room temperature in sealed vials and were then placed in an oil bath at a given temperature until the gel state was reached.

Gelation times were first measured by the tube tilting method. Sealed tubes containing the solutions (diameter 12 mm) at various concentrations are tilted and the gelation time is determined when no macroscopic flow is observed. In the given experimental conditions this method gives repeatable results. However, the determined gelation time depends on the size or shape of the sample tube, as gelation is determined in the nonlinear regime with this method. Actually, the apparent gel point is observed when the yield stress value of the gel exceeds the gravitational stress applied to the sample. Gelation times shown in Section 5 have been determined by linear rheology. While the trends are qualitatively similar, there is a consistent discrepancy by a factor of about 4–5 between each determination of the gelation time.

## 2.2 | Small-angle X-ray scattering

SAXS measurements were performed at the SWAXS laboratory (IRAMIS, Saclay, France) equipped with a two-dimensional detector. The acquisition time was 15 min. The  $q$  range extends from  $10^{-2}$  to  $0.5 \text{ \AA}^{-1}$ . Samples were placed in a closed cell in between two thin Kapton windows. The sample thickness was 1 mm. The electron density  $\rho_e^{(P)}$  [expressed as number of electrons, or electron units (e.u.), per  $\text{mm}^3$ ] of P(VDF-co-HFP) was estimated as an average over the electron densities of each segment, assuming a fraction of HFP of 20 mol% and a value for the copolymer density  $\rho \simeq 1.78 \text{ g/cm}^3$ . This estimate gives  $\rho_e^{(P)} \simeq 5.19 \times 10^{20} \text{ e.u./mm}^3$ . The electron density of MEK ( $\rho = 0.805 \text{ g/cm}^3$ ) is  $\rho_e^{(S)} = 2.683 \times 10^{20} \text{ e.u./mm}^3$ . For 2-heptanone ( $\rho = 0.82 \text{ g/cm}^3$ ), it is  $\rho_e^{(S)} = 2.762 \times 10^{20} \text{ e.u./mm}^3$ . These values give differences in electron density  $\Delta\rho_e = \rho_e^{(P)} - \rho_e^{(S)} \simeq 2.4$  to  $2.48 \times 10^{20} \text{ e.u./mm}^3$ . The electron coherent cross-section (Thompson scattering) shall be denoted  $\beta^2 = 7.9 \times 10^{-26} \text{ mm}^2$ .

## 2.3 | Large amplitude oscillatory shear

Small amplitude and Large Amplitude Oscillatory Shear (LAOS) experiments were performed at Laboratory of the Future (Bordeaux, France) on a Kinexus rheometer (Anton Paar) with a cone-plate geometry (CP4/40: angle  $4^\circ$  and diameter of 40 mm) and an enclosure containing a ring shaped solvent reservoir near the sample to prevent evaporation of the solvent. Samples were introduced in

the liquid state on the lower plate preheated at  $75^\circ$  and cooled down to the desired temperature at a heating rate of about  $60^\circ\text{C/min}$ .

Small amplitude measurements were performed to determine the gelation times and gel melting temperatures of the samples. The temperature was set in the range  $25\text{--}75^\circ\text{C}$ . The frequency was set at 1 Hz and the target shear strain at 0.1%, after performing a strain amplitude sweep to properly determine the linear regime. From these experiments the storage  $G'$  and loss  $G''$  shear moduli were recorded as a function of time and temperature.

To further assess the elastic response of the gel samples, oscillatory frequency sweeps were performed over the frequency range 0.1–10 Hz at 25 and  $75^\circ\text{C}$  with a fixed shear strain amplitude 0.1%.

## 3 | RESULTS

### 3.1 | Thermal gelation

The evolution of the complex shear modulus ( $G'$ ,  $G''$ ) as a function of time over a period of 1 h at  $T = 25^\circ\text{C}$  for the P(VDF-co-HFP) solution in 2-heptanone with  $\Phi_P = 10 \text{ wt}\%$  is shown in Figure 2. Starting from the liquid state at time  $t = 0$ , with  $G''$  much higher than  $G'$  (in fact  $G'$  is hardly measurable in the chosen cone-plate configuration), the complex modulus evolves drastically as a function of time, with  $G'$  increasing considerably to reach values well above  $G''$ , which indicates that the sample has changed from a liquid state to an elastic state. Note that the system still continue to evolve over a long time scale.

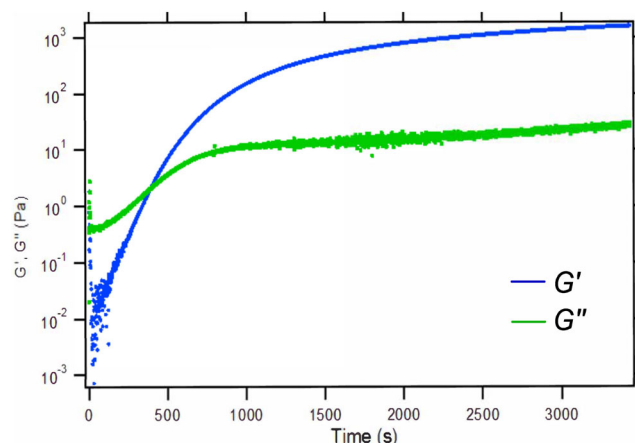


**FIGURE 2** The storage ( $G'$ , blue curve) and loss ( $G''$ , green curve) linear moduli as a function of time during the gelation of P(VDF-co-HFP) solution in 2-heptanone with  $\Phi_P = 10 \text{ wt}\%$  at  $25^\circ\text{C}$ , at a frequency 1 Hz and strain amplitude 0.1%



The complex modulus still increases slowly in an apparent logarithmic way.

Gelation is further assessed by measuring the variation of the modulus as a function of the frequency in the gel state, after 1 h delay. As shown in Figure 3,  $G'$  is independent of the frequency within the investigated frequency range. This indicates that the system possess some permanent elastic response in the time range corresponding to the measured frequency window. Figure 3 also shows that at 100 °C, that is, above the gelation temperature, the complex modulus depends on the frequency, with qualitative

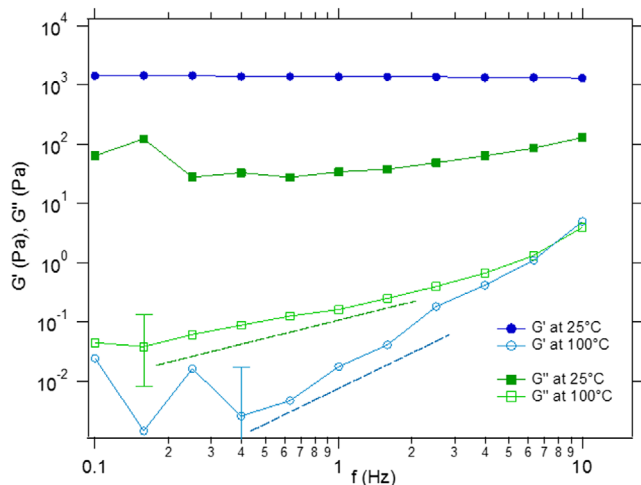


**FIGURE 3** The storage  $G'$  (blue circles) and loss  $G''$  (green squares) linear moduli as a function of frequency in the gel state (after 1 h time sweep), for P(VDF-co-HFP) solution in 2-heptanone with  $\Phi_P = 10$  wt% at 25 °C, at a strain amplitude 0.1%. Full symbols:  $T = 25$  °C (below the gelation temperature); hollow symbols  $T = 100$  °C (above gelation temperature)

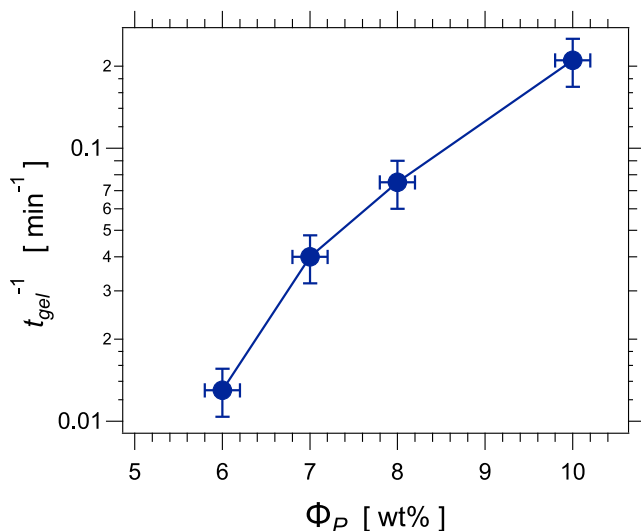


**FIGURE 4** The gelation rate  $t_{\text{gel}}^{-1}$  as a function of the copolymer concentration  $\Phi_P$  at 25 °C in 2-heptanone

variations corresponding roughly to  $G' \sim f^2$  and  $G'' \sim f$ , which corresponds to the behavior of a viscous liquid.

The gelation time  $t_{\text{gel}}$ , or equivalently the gelation rate  $1/t_{\text{gel}}$ , may be conveniently defined as the time when  $G'$  and  $G''$  curves cross. The gelation rate at  $T = 25$  ° is plotted as a function of the copolymer concentration for the solutions in 2-heptanone in Figure 4. Figure 4 shows that the gelation rate (or equivalently gelation time) strongly depends on the copolymer concentration. It varies between about 80 min and about 4 min as the concentration changes from 6% to 10%.

The behavior of the solutions of poly(VDF-co-HFP) copolymer in MEK is qualitatively similar, but drastically different in terms of gelation time in the same concentration range. Gelation is typically three orders of magnitude slower in MEK than in 2-heptanone. Besides, a copolymer solution in MEK does not gelify within a measurable time scale at room temperature below about 15%, while in heptanone this threshold seems to be lower than 2%.

### 3.2 | Large-scale structure: Small-angle X-ray scattering

As the electron density of the fluorinated copolymer and those of the solvents are significantly different (electron density differences  $\Delta\rho_e = \rho_e^{(P)} - \rho_e^{(S)}$  of about 2.4 to  $2.48 \times 10^{20}$  e.u./mm<sup>3</sup>), there is a strong contrast between the copolymer and the solvent, and SAXS is an appropriate technique to obtain pieces of information on the structure of the system, namely, concentration heterogeneities at various scales, specifically in the gel state, in the same way as when neutron scattering is used with deuterated polymers in solution.<sup>37</sup>

Due to the overall long gelation time scales and high concentration thresholds for gelation, we first show scattering results from copolymer solutions in MEK, as this allows easy comparison between liquid solutions and gels. The scattered intensities measured for P(VDF-co-HFP)-MEK solutions at different concentrations are shown in Figure 5. In liquid solutions below the sol-gel transition [4 and 13 wt% of P(VDF-co-HFP)] the scattering is typical of a single-phase polymer-solvent mixture, with small concentration fluctuations. The scattering intensity starts increasing at very small angle in the system with 15 wt% of P(VDF-co-HFP), which is very close to the gel point. This indicates the presence of weak, large-scale heterogeneities in the system. Above the sol-gel transition (gel corresponding to 20 and 26 wt% of P(VDF-co-HFP) in Figure 5), the scattering patterns change and qualitatively new features appear. Below a critical  $q_c$  value of about  $0.1 \text{ \AA}^{-1}$  typically, large

additional scattering appears, while above  $q_c$  the shape of the scattering does not change significantly. No correlation peak with a maximum at a finite  $q$  value is observed. The scattering intensity at low  $q$  values (below  $q_c$ ) increases as the polymer concentration increases, while keeping essentially the same shape. This scattering shape is typical of polymer-polymer or polymer-solvent phase separated systems with sharp interfaces, with a  $q^{-4}$  power law in the approximate range  $0.05 < q < 0.1 \text{ \AA}^{-1}$ . Such type of scattering has been observed in neutron scattering experiments on phase separating polymer blends.<sup>38–40</sup> More precisely, the fact that the scattering appears below a well-defined value  $q_c$  may indicate that phase separation occurs in the nucleation regime rather than in the spinodal regime. In the nucleation regime, there is a critical size  $r_c$  below which a nucleated droplet of the phase will vanish, while above  $r_c$  it will grow. Thus all phase-separated domains which grow as the system undergoes phase separation are larger than  $r_c$ , which gives a scattering only at  $q$  values smaller than  $q_c \approx 2\pi/r_c$ . Based on the observed  $q_c$  value, the estimated  $r_c$  should be of order 6 nm.

However, this typical scale  $r_c \approx 6 \text{ nm}$  probed by SAXS here is about 10 times smaller than that observed in phase separating polymer blends.<sup>38–40</sup> It is also much smaller than typical scales associated to phase separation in polymer solutions and other soft systems, often occurring in the spinodal regime, which are of order a few  $\mu\text{m}$  up to tens of  $\mu\text{m}$ .<sup>41</sup> Note also that the gels remain fully transparent. Therefore, the observed scattering should be

associated to some local structure at the nanometer scale formed by the copolymer as the very early stage of phase separation. This local structure, be it related to self-assembly of the copolymer and/or to crystallization, shall then play the role of network junctions and prevent further evolution of the minority polymer-rich phase into isolated droplets, preserving a three-dimensional network.

Below  $q_c$ , the scattering may be semiquantitatively described by the Debye–Bueche equation.<sup>37</sup>

$$I(q) = \beta^2 (\Delta\rho_e)^2 \varphi(1-\varphi) \frac{\xi^3}{(1+q^2\xi^2)^2}. \quad (1)$$

In Equation (1),  $\beta^2 (\Delta\rho_e)^2$  is the contrast factor, where  $(\Delta\rho_e)^2 = (\rho_e^{(P)} - \rho_e^{(S)})^2$  is the electron density difference between the polymer-rich phase and the solvent,  $\varphi$  is the volume fraction occupied by one of the phases (e.g., the polymer-rich phase) and  $\xi$  the characteristic size of the structure. This equation describes domains of the coexisting phases (one rich in polymer and one rich in solvent) with sharp interfaces. Examples of fits are shown in Figure 5. They were obtained with the domain size value  $\xi = 3.6 \text{ nm}$ .

To illustrate the effect of concentration, the scattered intensities measured for P(VDF-co-HFP)—2-heptanone mixtures at different concentrations are shown in Figure 6. As gelation times in heptanone are quite fast, these curves can be considered as corresponding to the final states of the gels. The curves are qualitatively similar to those obtained in MEK. The scattered intensities

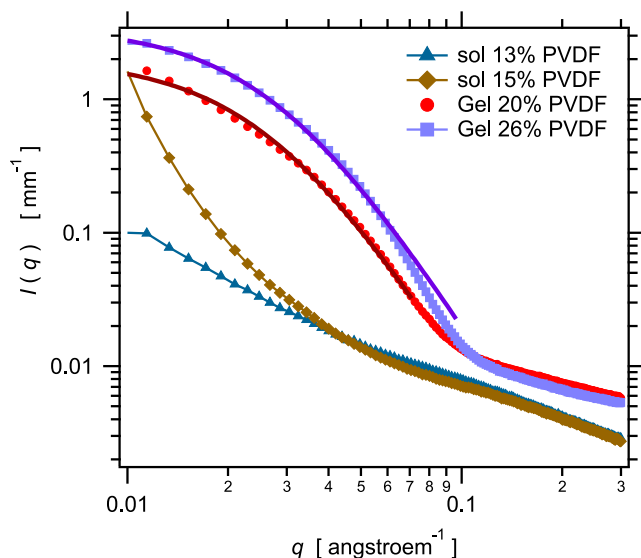


**FIGURE 5** Normalized SAXS profiles for P(VDF-co-HFP)—MEK systems with different fractions of P(VDF-co-HFP): Light blue:  $\Phi_P = 4 \text{ wt\%}$ ; blue:  $\Phi_P = 13 \text{ wt\%}$ ; brown:  $\Phi_P = 15 \text{ wt\%}$ ; red:  $\Phi_P = 20 \text{ wt\%}$ ; violet:  $\Phi_P = 26 \text{ wt\%}$ . The systems with  $\Phi_P = 20$  and  $26 \text{ wt\%}$  are in the gel state. The blue and red curves are fits with Equation (1)

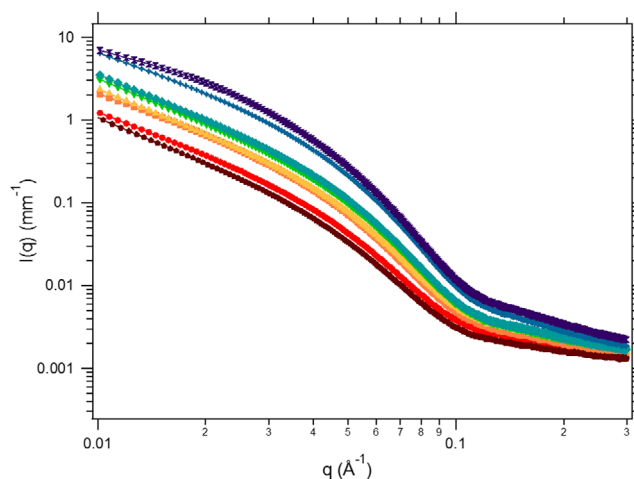


**FIGURE 6** Normalized SAXS profiles for P(VDF-co-HFP)—2-heptanone systems with different weight fractions of P(VDF-co-HFP): Brown symbols:  $\Phi_P = 2 \text{ wt\%}$ ; red bullets:  $\Phi_P = 3 \text{ wt\%}$ ; orange squares:  $\Phi_P = 4 \text{ wt\%}$ ; yellow triangles:  $\Phi_P = 5 \text{ wt\%}$ ; green down triangles:  $\Phi_P = 6 \text{ wt\%}$ ; blue diamonds:  $\Phi_P = 7 \text{ wt\%}$ ; dark blue symbols:  $\Phi_P = 15 \text{ wt\%}$ ; black symbols:  $\Phi_P = 20 \text{ wt\%}$

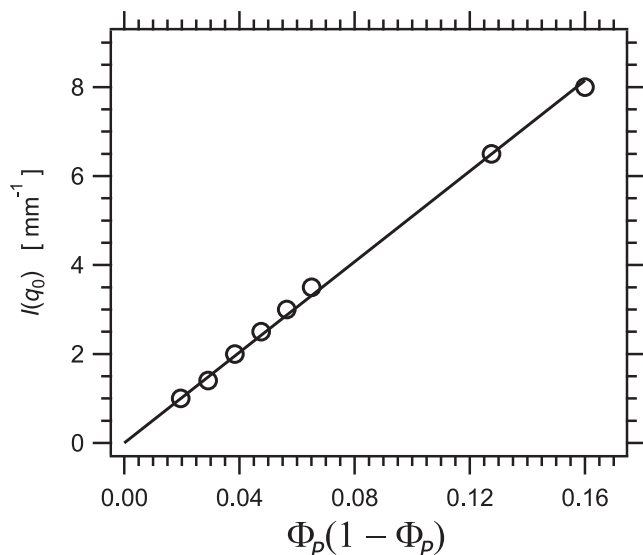


**FIGURE 7** The intensities of the curves shown in Figure 6, taken at  $q_{\min} = 0.01 \text{ \AA}^{-1}$ , as a function of the factor  $\Phi_p(1 - \Phi_p)$  where  $\Phi_p$  is the polymer concentration in the initial solution

increase below a well-defined  $q_c$  value of the order  $q_c = 0.11 \text{ nm}^{-1}$  which corresponds to a structure size of the order  $r_c \approx 2\pi/q_c \approx 6 \text{ nm}$ , independent of the concentration. The general shape of the scattering curves does not depend on the concentration either. These observations confirm that an identical local structure is formed, independent of the initial copolymer concentration.

The scattered intensity increases as the polymer concentration increases. According to Equation (1), the scattered intensity should be proportional to  $\varphi(1 - \varphi)$  where  $\varphi$  is the volume fraction occupied by the polymer-rich phase. However, what is known is  $\Phi_p$ , the overall polymer concentration in the initial solution, not  $\varphi$ . By neglecting the amount of polymer contained in the solvent-rich domains, it may be assumed that  $\varphi$  is proportional to  $\Phi_p$ . The scattered intensity, arbitrarily measured at  $q_{\min} = 0.01 \text{ \AA}^{-1}$ , plotted as a function of the factor  $\Phi_p(1 - \Phi_p)$  is shown in Figure 7. A linear variation is observed, which is in agreement with Equation (1).

The slope of the linear adjustment in Figure 7 is of order  $50 \text{ mm}^{-1}$ . According to Equation (1), this slope should be roughly equal to  $\beta^2 \Delta \rho^2 \xi^3$  where  $\xi$  is the typical size of the phase-separated domains [assuming  $(q_{\min} \xi)^2 \ll 1$ ]. By assuming an electron density difference  $\Delta \rho_e \approx 2 \times 10^{20} \text{ e.u./mm}^3$  and  $\xi = 5.5 \text{ nm}$ , a value  $50 \text{ mm}^{-1}$ , equal to the measured one (the slope of the line in Figure 7), is obtained. Altogether, this indicates that the measured scattered intensities are roughly coherent with Equation (1), assuming that copolymer structures of size 5–6 nm are present, within a very diluted solvent-rich phase and with an overall volume fraction comparable to the initial copolymer concentration.

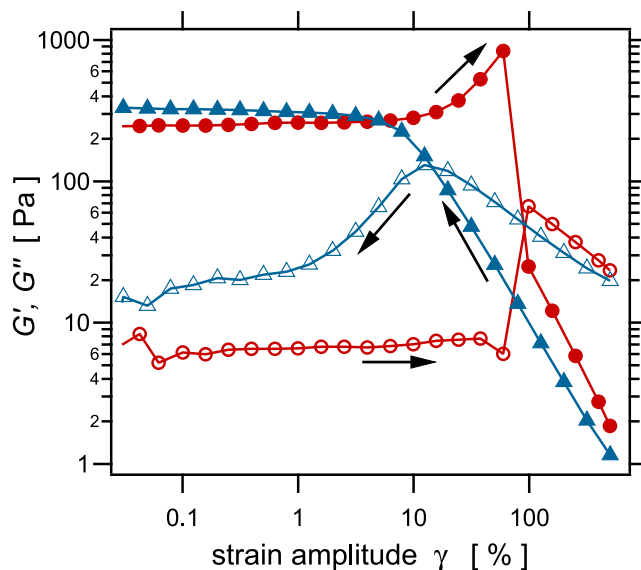


**FIGURE 8** The shear modulus as a function of the LAOS strain amplitude for a P(VDF-co-HFP)—2-heptanone gel at  $\Phi_p = 7 \text{ wt\%}$ . Red circles: Upwards strain ramp, 0.01% up to 500%; blue triangles: Downwards strain ramp, 500% down to 0.01%. Filled symbols:  $G'$ ; empty symbols:  $G''$ . Experiments were performed at  $25^\circ \text{C}$  and a frequency of  $1 \text{ Hz}$

### 3.3 | Nonlinear rheological response of thermoreversible gels

The nonlinear rheological properties of the P(VDF-co-HFP) physical gels in 2-heptanone using LAOS experiments are described in this Section. Results obtained in gels in 2-heptanone only are reported, as reliable results could not be obtained in gels in MEK due to solvent evaporation in the course of the measurements. We shall concentrate on systems between 6 and 10 wt% of copolymer, which have gelation times typically between about 5 min and about 1 h (see Figure 4). The rheological behavior of the gels under LAOS was measured after performing a 1-h time sweep and a frequency sweep to check the gel state of our materials, as described in Section 5.

An example of the evolution of the viscoelastic moduli  $G'$  and  $G''$  of a P(VDF-co-HFP)—2-heptanone gel with  $\Phi_p = 10 \text{ wt\%}$  as a function of the strain amplitude is shown in Figure 8. At low strain amplitude, both the storage and loss moduli remain constant, characteristic of the linear viscoelastic (LVE) regime and  $G'$  is higher than  $G''$  which assesses the elastic-like behavior of the material (gel state). On increasing the strain amplitude above about  $\gamma = 5\%$ , the value of the elastic modulus  $G'$  increases quite sharply, that is, the system exhibit strong strain hardening. As the strain amplitude reaches a critical value ( $\gamma = 57\%$  in the example shown in Figure 8),



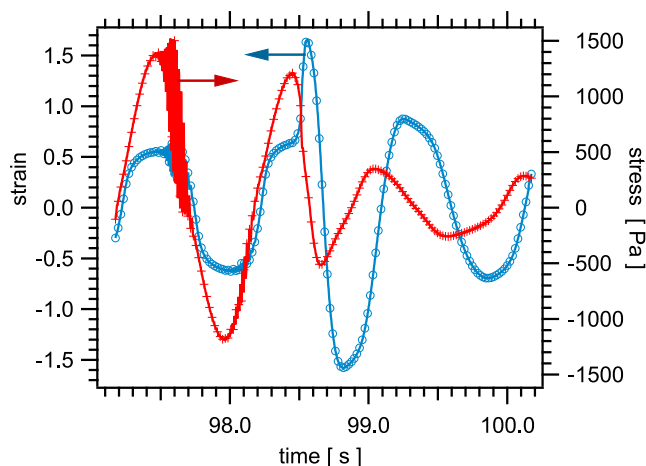


**FIGURE 9** Stress (red crosses) and strain (blue circles) as a function of time in P(VDF-co-HFP)—2-heptanone gel with  $\Phi_p = 7$  wt% during three periods of oscillation, at high strain amplitude. At the beginning of the time window which is shown, the system is elastic. The stress is nearly in phase with the strain and the stress is of order 1.5 kPa (modulus  $G'$  of order 2 kPa). Some high-frequency stress oscillations appear just before the abrupt transition towards the viscous regime, which occurs here at about 98.5 s. In the subsequent viscous regime, the stress is nearly in phase with the strain rate (i.e., in quadrature with the strain)

the elastic modulus  $G'$  then drops abruptly to a very small value while the loss modulus  $G''$  rises above  $G'$ . Above  $\gamma = 100\%$ , the loss modulus  $G''$  stays higher than  $G'$ , meaning that the system is in the viscous (liquid) state.

In a subsequent step, the strain amplitude was progressively decreased back to the linear regime, from 500% down to 0.1%. The corresponding curves for the elastic and loss moduli are shown in Figure 8, superimposed on the curves for the upwards strain sweeps. Final values of the moduli very close to the initial ones are recovered when the linear regime is reached back, meaning that the elastic-to-viscous transition is reversible. However, the behavior during the downwards ramp does not superimpose on that for the upwards ramp. The curves corresponding to the downwards strain sweep are continuous and monotonous. No strain-hardening phenomenon is detected during the downwards sequence. The system seems to evolve progressively from a viscous state to an gel-like, elastic state. The sol–gel transition, determined as the crossing point between  $G'$  and  $G''$ , occurs around  $\gamma \approx 10\%$  on decreasing the strain amplitude, while the system stays elastic up to  $\gamma \approx 80\%$ –100% on increasing the strain amplitude.

The points at which the systems suddenly lose their elasticity may be dependent on the experimental conditions. There may be a critical stress level for either internal fracture or for onset of slippage at the cell walls. This precise value should then not be considered as

representative of an intrinsic property of the material. Figure 9 shows real time recording of the elastic breakdown. Some high-frequency stress oscillations, possibly associated to stick–slip at the walls of the measuring cell or to sporadic propagation of a crack or elastic defect, develop just before the transition to liquid flow suddenly occurs. Note that the breakdown occurs at a point where the stress is close to be maximum.

The nonlinear behavior is further shown in Figure 10. At small strain amplitudes, in the linear regime, the response is nearly fully elastic, with a loss factor  $G'/G'' = \tan\delta$  of order 0.03 (see also Figure 8). On entering the nonlinear regime, stress–strain curves show a pronounced strain hardening effect, while still keeping a very low loss factor, as measured by the inner area of the stress–strain cycles as compared with the stored mechanical energy. As the system undergoes the abrupt transition to the liquid state, the cycles become characteristic of a nonlinear, viscous fluid. On the downwards strain sweep, the stress–strain cycles evolve progressively from viscous to elastic, as illustrated also in Figure 10.

In another series of experiments, a time sweep at fixed frequency and small shear strain was carried out immediately after shearing at high amplitude, when the sample is in the liquid state. This experiment was performed to measure the complex modulus as a function of time and determine the time for recovery of the initial gel behavior at rest after LAOS experiment. As shown in Figure 11, the gelation of P(VDF-co-HFP)—2-heptanone is almost instantaneous. The system recovers a complex modulus nearly identical to the initial one within a couple of seconds. This evolution is very different from the gelation induced by thermal treatment, in which the gelation time at rest was around 500 s in the same sample (see Figure 3). This result shall be further discussed in Section 4.

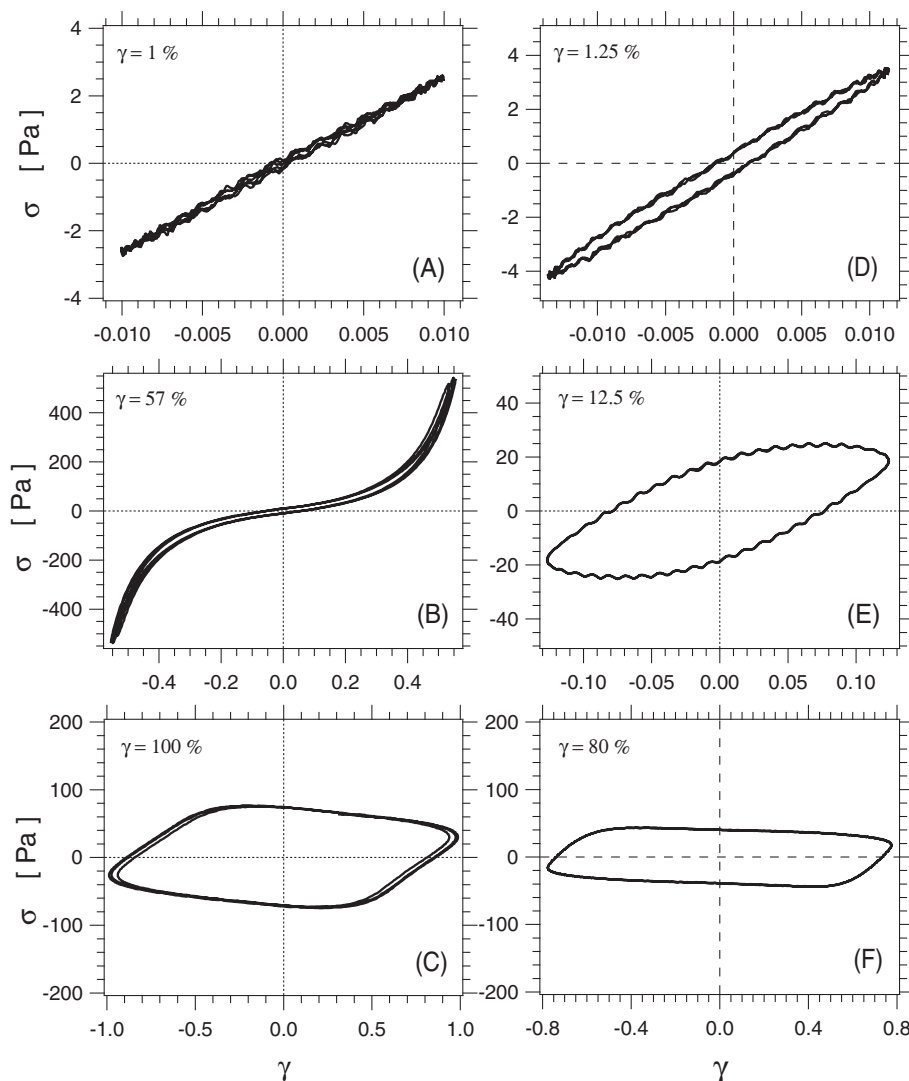
The nonlinear response of the gels was investigated for systems between 6 and 20 wt% of copolymer. All systems show qualitatively similar behavior, with comparable strain hardening and abrupt transition from an elastic towards a viscous liquid behavior at comparable values of the strain and/or the maximum stress.

## 4 | DISCUSSION

### 4.1 | Phase separation

MEK and heptanone are not very good solvents of the P(VDF-co-HFP) copolymer. Flory interactions parameters have been estimated for a number of different solvents, including ketones of various chain lengths, at temperatures higher than room temperature however.<sup>12,42</sup> It was found that ketone solvents of various chain lengths have

**FIGURE 10** LAOS stress–strain (Lissajou) curves on a P(VDF-co-HFP)—2-heptanone gel with  $\Phi_P = 7$  wt%. Left column (A–C): Upwards strain ramp; right column (F–D): Downwards strain ramp. Experiments were performed at 25 °C and a frequency of 1 Hz. Strain amplitudes  $\gamma$  are indicated. The small amplitude, high-frequency modulation visible in (A), (D), and (E) is due to the limited signal-to-noise of the rheometer in the chosen geometry and to small artifacts in signal treatment



$\chi$  Flory interaction parameters in the vicinity of 0.5 near room temperature, the value being closer to 0.5 as the chain length increases up to heptanone. It was found that PVDF/ketone solvent systems indeed undergo thermoreversible gelation. Note that the interaction parameter may be further affected by the presence of HFP comonomers as compared with PVDF.

Alternatively,  $\chi$  Flory interaction parameters may be estimated from solubility parameters using the Hildebrand equation:

$$\chi = \frac{(v_S v_P)^{1/2}}{RT} (\delta_P - \delta_S)^2, \quad (2)$$

where  $v_S$  and  $v_P$  are the molar volumes of the solvent molecule and the monomer, respectively, and  $\delta_S$  and  $\delta_P$  are the solubility parameters of the solvent and the polymer.  $\delta_P$  and  $\delta_S$  are estimated by taking into account the three Hansen components according to  $\delta^2 = \delta_{(d)}^2 + \delta_{(p)}^2 + \delta_{(h)}^2$ ,  $\delta_{(d)}$ ,  $\delta_{(p)}$ , and  $\delta_{(h)}$  being the dispersive, polar

and hydrogen bond contributions, respectively. However, given the large variations in values reported in the literature,<sup>42–45</sup> it is very difficult to give reliable estimate of the Flory interaction parameters of PVDF with MEK and with heptanone, without even mentioning the presence of the HFP comonomers, which may further affect its value. Nevertheless, the following qualitative arguments can be stated as regards the relative solvent quality of MEK and heptanone for PVDF. Reported values of the total solubility parameter  $\delta_P$  of PVDF range from 19.2 to 23.2 MPa<sup>1/2</sup>.<sup>42,43</sup> For MEK, the total solubility parameter  $\delta_S$  is in the range 18.35–19 MPa<sup>1/2</sup>.<sup>42,43</sup> For heptanone it should be smaller than this value, whatever the way by which it is estimated, because the molar volume is larger (about 140 cm<sup>3</sup>/mol for heptanone vs. about 90 cm<sup>3</sup>/mol for MEK) and the molecule is less polar than MEK. The solubility parameter for heptanone was estimated to be in the range 17.6–18.2 MPa<sup>1/2</sup> based on the group contribution method using Van Krevelen group values.<sup>44,45</sup> From the estimated values reported above, the Flory

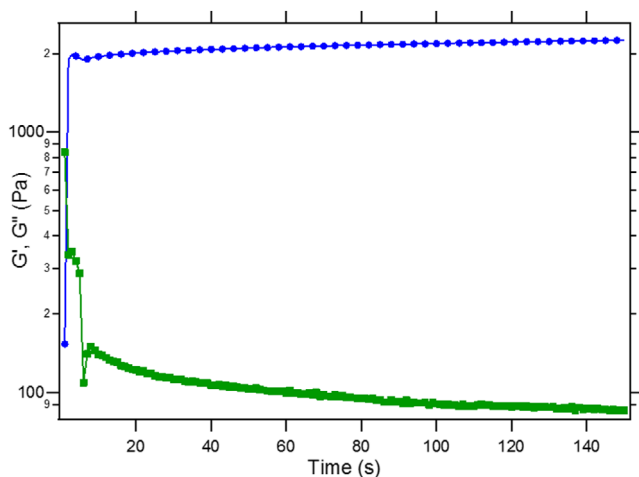


**FIGURE 11** Evolution of the viscoelastic shear moduli  $G'$  and  $G''$  as a function of time as the strain is stopped after LAOS measurement on a P(VDF-co-HFP)—2-heptanone gel with  $\Phi_P = 10$  wt% of copolymer. Experiments were performed at 25 °C and a frequency of 1 Hz. The material recovers its elastic behavior within a couple of seconds

interaction parameter might be around 0.41 for PVDF/MEK and 0.6 for PVDF/heptanone. Besides, as noted above, a further source of uncertainty comes from the presence of the HFP comonomers. The systems may then be in the metastable region of the phase diagram, indicating that phase separation would occur through a nucleation mechanism, which is coherent with SAXS observations. PVDF/heptanone solutions are more prone to phase separation, with a higher nucleation rate, which is also coherent with observed much faster gelation rates.

Phase separation in polymers and viscoelastic systems has been extensively discussed in the seminal work of Tanaka.<sup>41</sup> In particular, it was shown that the more viscoelastic phase forms a continuous network structure in order to support the local stress. This may certainly correspond to the present case, in which the polymer-rich phase may form a continuous network responsible for the gel-like, elastic response of the system, even though it is the minority phase, in agreement with case (b) in Figure 25 of Reference [41]. However, the early formation of copolymer structures (possibly crystallites) at the nanometer scale, inhibits further growth of phase-separated domains over larger scale.

## 4.2 | Strain hardening

Gels stiffen as they are strained. Strain-hardening is observed at approximately 50% of deformation. It manifests itself in two ways. First, the apparent elastic modulus plotted as a function of the strain amplitude (see

Figure 8) increases; second, stress-strain cycles at increasing strain amplitudes exhibit increasingly pronounced strain hardening (see Figure 10B).

Strain-hardening has been observed in various materials including polymer gels and more particularly biopolymer gels made of DNA,<sup>46</sup> gelatin,<sup>47</sup> or cellulose<sup>48</sup> for example. However, to our knowledge, the linear and non-linear behavior of PVDF gels has not been thoroughly studied.<sup>17</sup> In DNA gels, strain-hardening was attributed to finite extensibility of DNA double-strand chains forming the gel, which have a very long persistence length, that is, are quite rigid.<sup>46</sup> For gels made of flexible chains, finite extensibility would not be observed in the range of deformation which is studied. Let us make this argument more precise.

For a homogeneous gel made of very flexible chains, the elastic modulus in the linear regime would be expressed as

$$G \approx nRT \approx \left( \frac{\rho\phi}{M_c} \right) k_B T, \quad (3)$$

where  $n$  is the number of elastic chains (twice the number of crosslink points for tetrafunctional crosslinks) per unit volume,  $\rho$  the density of P(VDF-co-HFP),  $\phi$  the polymer volume fraction and  $M_c$  the average molar mass between crosslinks.

Considering  $\rho = 1.78 \times 10^3$  kg/m<sup>3</sup>,  $\phi = 6$  vol%,  $G = 10^3$  Pa at  $T = 313$  K, we find  $M_c \approx 278$  kg/mol, which corresponds roughly to 4500 monomers and to a number of segments  $N \approx 500$ . Stated in another way, such a very small elastic modulus would correspond to a very loose network with a very low crosslink density. Remember that typical elastomer moduli are in the range of a few hundreds of kPa up to about 1 MPa.

The force-extension curve of a flexible chain of  $N$  Kuhn segments of length  $a$  is given by:

$$f = \frac{k_B T}{a} L^{-1} \left( \frac{R}{Na} \right), \quad (4)$$

where  $f$  is the force exerted on chain ends and  $R$  is the end-to-end vector of the chain.  $L^{-1}(x)$  is the inverse of the Langevin function  $L(x) = \text{ch}x/\text{sh}x - 1/x$ . In this expression the force  $f$  diverges as  $R$  reaches the maximum extension  $R_{\max} = Na$  (fully stretched chain). To make a parallel with the behavior of a stretched macroscopic system such as a gel, an equivalent “elongation ratio”  $\lambda$  can be defined as  $R/\langle R_0^2 \rangle^{1/2}$  where  $\langle R_0^2 \rangle \approx Na^2$  is the squared equilibrium “length” of a chain. Thus the fully stretched state would correspond to an extension ratio of order  $N^{1/2}$ . It follows that strain-hardening related to finite extensibility would occur at typical (elongation)

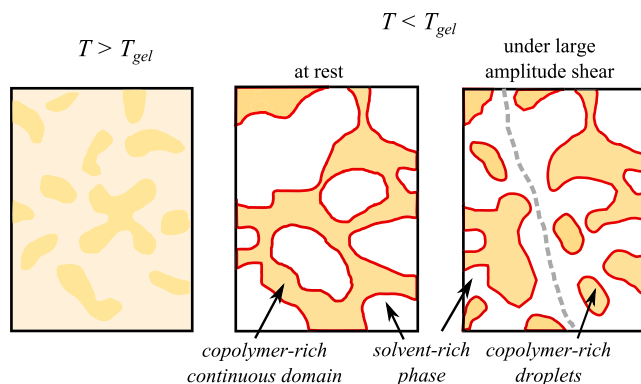


**FIGURE 12** Schematics of the proposed mechanism for the nonlinear behavior of P(VDF-co-HFP)—2-heptanone gels. Above the critical gelation temperature  $T_{gel}$ , the system is homogeneous (with concentration fluctuations). Below  $T_{gel}$ , the system phase-separate. Under large amplitude shear, the continuous, elastic polymer-rich domain is broken and elasticity is no longer transmitted along a fracture (as schematized by a gray dashed path)

strain values of order  $N^{1/2}$  which amounts to about 20–25 by taking  $N \approx 500$  and is much larger than what is observed. Conversely, to observe large strain-hardening effect in the range of 100% elongation, one should have a value of  $N$  of order 2, which means unrealistically short and/or rigid chains in the gel network.

Therefore, explaining such a high strain-hardening effect in the gels studied here is not easy. P(VDF-co-HFP) chains in solvent are certainly not semirigid as it is the case for double-strand DNA.<sup>46</sup>

We may speculate that a picture which would be coherent with other observations (namely, SAXS) and considerations about the Flory parameter of the solvent, is a partially segregated, polymer-rich network within a solvent-rich phase as schematized in Figure 12. Note that the scheme at rest in Figure 12 is similar to that proposed by Tanaka in Figure 25(b) in Reference [41]. The elasticity would then be transmitted only through the polymer-rich domain. In this domain, the density of effective crosslinks (entanglements, crystallites...) could be much higher than the overall average value estimated above. This could lead to much enhanced strain-hardening effect.

To describe the strain-hardening in a more quantitative way, we propose to analyze the stress–strain curves obtained in the elastic regime in more details (see Figure 10). We first use the method proposed by Cho et al. to extract a purely elastic component of the stress.<sup>49,50</sup> This component is the one which is in phase with the strain (while the viscous part is in phase with the strain rate). Writing the oscillatory strain as  $\gamma(t) = \gamma_0 \sin(\omega t)$ , that is, as an odd function of the time  $t$ , the elastic part of the stress shall then be the odd part of

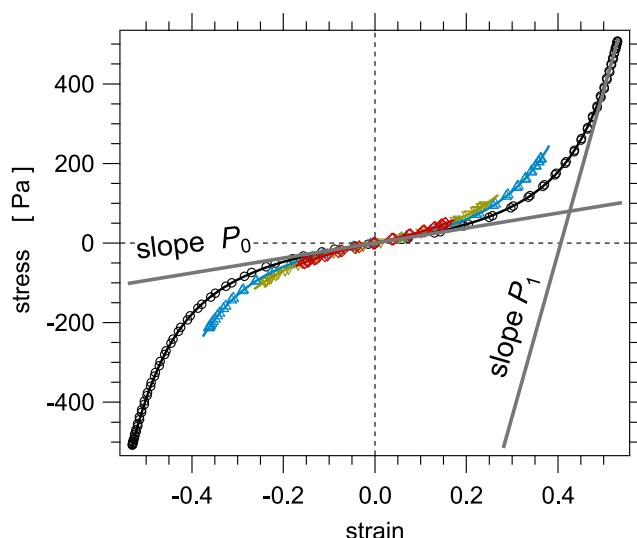


**FIGURE 13** The purely elastic contributions  $\sigma_{el}$  to the stress–strain cycles for a P(VDF-co-HFP)—2-heptanone gel with  $\Phi_P = 7$  wt% and amplitudes from  $\gamma = 15\%$  up to about 52%. Symbols: Analyzed elastic data; curves: Polynomial fits as described in the text. The determination of the  $P_0$  and  $P_1$  slopes of  $\sigma_{el}$  used for the calculation of the strain-hardening ratio  $H = P_1/P_0$  is illustrated

the stress, which may be simply computed as  $\sigma_{el} = (\sigma(t) - \sigma(-t))/2$ , or equivalently  $\sigma_{el} = (\sigma(t) - \sigma(T_{osc} - t))/2$  where  $T_{osc}$  is the period of the oscillatory strain.

The hysteresis (the difference between up and down branches of the original cycle) is quite small in the whole hyperelastic regime, which means that the gels have very low dissipation (see a representative example in Figure 10B). Examples of nonlinear elastic response curves obtained by this procedure are shown in Figure 13 for a P(VDF-co-HFP)—2-heptanone gels with 7 wt% of copolymer, for strain amplitudes between about 0.15 and 0.57. By definition, computing the purely elastic stress  $\sigma_{el}$  cancels the hysteresis.

The shape of the elastic response curve is qualitatively similar to an inverse Langevin function. It cannot be fitted quantitatively with this function, though. Note anyway that the inverse Langevin function describes finite extensibility of a single chain submitted to axial simple extension, while the deformation mode applied here is shear.

To describe the nonlinear behavior of gels and rubber-like materials, a nonlinear strain energy function was proposed by Groot et al.<sup>47</sup> in the form of a series expansion of the first strain invariant  $I_1$ , using the generalized empirical nonlinear expression  $I_1 = (\lambda^n + \lambda^{-n})/n$  where  $\lambda$  is defined by  $\gamma = \lambda - \lambda^{-1}$  with  $\gamma$  the shear angle.<sup>51</sup> The linear constitutive law corresponds to one single term in the expansion and to  $n = 2$ . The resulting

overall hyperelastic constitutive equation is a polynomial of the form  $\sigma_{el} = \sum_{k=1}^{\infty} C_k \gamma^k$  with  $k$  taking odd values ( $k = 1, 3, 5$ , and so forth). Note that  $C_1 = G$  is the linear shear modulus. An example of such fit is shown in Figure 13.

We then introduce a parameter (strain-hardening ratio)  $H$  defined as the ratio:

$$H = \frac{P_1}{P_0}, \quad (5)$$

where  $P_1$  is the slope at the maximum of  $\sigma_{el}$  and  $P_0$  the slope of  $\sigma_{el}$  at the origin (i.e., the elastic modulus of the gel). These slopes are shown for the example shown in Figure 13. The values of  $P_1$  and  $P_0$  and thus the strain-hardening ratios have been determined for each value of strain amplitude during the upwards ramp of the LAOS experiments.

The slope  $P_0$  start to decrease moderately as the strain amplitude increases beyond typically 0.25, which indicates that the gels have some degree of plasticity. Nevertheless the behavior is characteristic of a nearly purely elastic behavior. This is quite different from the Payne effect observed in reinforced elastomers, in which the modulus decreases significantly as the strain amplitude increases in the nonlinear regime.<sup>50</sup> Note also that the apparent increase of modulus shown in the upward (red) curve in Figure 8 is actually due to strain hardening and not to an increase of the slope  $P_0$  as the strain amplitude increases.

The strain-hardening ratio  $H$  was determined for P(VDF-co-HFP)—2-heptanone gels with concentrations of copolymer between 6 and 10 wt%. Its evolution as a function of the strain amplitude during the upwards ramp of the LAOS experiment at different concentrations of copolymer is shown in Figure 14. Considering the previously mentioned hyperelastic constitutive equation and derivating it, and neglecting plasticity effects, the ratio  $H$  should be expressed as a function  $H = 1 + h_2\gamma^2 + h_4\gamma^4 + \dots$ , where  $\gamma$  is the strain amplitude. The curve in Figure 14 corresponds to  $H = 1 + 22\gamma^2 + 110\gamma^4$ . This curve should be understood as a guide for the eyes, as it is purely heuristic.

Figure 14 suggests that the strain hardening ratio is roughly independent of the gel concentration, even though the elastic moduli in the linear regime vary by about one order of magnitude over the investigated concentration range, as shown in inset in Figure 14. Among polymer/solvent systems reported in the literature, only biopolymer gels such as, for example, gelatin, alginate, or DNA gels, show comparable degree of strain hardening,<sup>46,51,52</sup> with quite low initial modulus and steep increase of the stress. The nonlinear mechanical behavior of gels with stiff, rod-like junctions has been

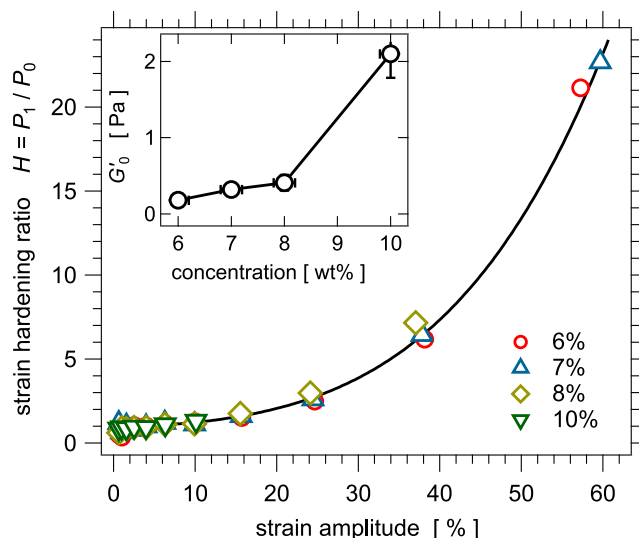


**FIGURE 14** Evolution of the strain-hardening ratio  $H = P_1/P_0$  as a function of the strain amplitude for P(VDF-co-HFP)—2-heptanone gels with different fractions of copolymer: Red circles: 6 wt%; blue triangles: 7 wt%; light green diamonds: 8 wt%; green down triangles: 10 wt%. The curve corresponds to a polynomial adjustment (see text) and is a guide for the eye. Inset: The elastic modulus in the linear regime as a function of the polymer concentration in the gel

described by Doi and Kuzuu.<sup>53</sup> Combining a linear variation at small amplitude and the strain-hardening contribution due to stiff junctions proposed by Doi and Kuzuu indeed gives a reasonable representation of the data. Thus, the observed behavior seems to indicate that polymer-rich regions behave in a similar way as rod-like effective crosslinks present in biopolymer gels.

### 4.3 | Recovery of elasticity after large amplitude shear

The gel-sol transition induced by increasing temperature is reversible. The gels recover values of viscoelastic moduli close to those measured before the temperature cycle. While the behavior of gels is often studied using single stress-strain curves at a given strain rate up to failure, here we have been considering the recovery after elastic failure in two distinct cases, either at rest immediately after large amplitude shearing or on decreasing progressively the strain amplitude back to zero.

Above the critical gelation temperature  $T_{gel}$ , the copolymer solution is in a single phase state, with concentration fluctuations. Below  $T_{gel}$ , the system phase separates. In the LVE region (for strain amplitude lower than 10%), the gels may be organized into solvent-rich and polymer-rich regions. In the polymer-rich zones, a polymer network would exist and polymer chains would



be crosslinked by physical junction points that are crystallites. When a deformation is applied in a nonlinear transient regime (for typically  $10\% < \gamma < 50\%$ ), the structure of the material evolves while remaining in the gel state.

When the strain amplitude continues to increase, the gel abruptly softens and shows a liquid-like response (for  $\gamma > 100\%$ ). This abrupt change of behavior should correspond to failure of the polymer-rich network, either through slippage at the wall or within the bulk of the gel.

The complete recovery of the initial elastic modulus after the downwards strain sweep suggests that the same material is formed (same fraction of physical junction points, same polymer-rich network). As judged from the rheological behavior, the material quite quickly loses the memory of the previous fracture.

Note that the material does not follow the same path on the upwards and downwards parts of the strain sweep (see Figure 8). On the downwards strain sweep, the evolution shows a monotonous evolution of the complex modulus and does not reproduce the strain-hardening behavior observed on the upwards sweep. We may speculate that the polymer rich zones on both sides of the fracture surface are able to reconnect progressively, leading to progressive, though fast enough, healing of the fracture. Figure 12 qualitatively illustrates a possible morphology of the gel in the vicinity of the fracture zone.

## 5 | CONCLUSIONS

In this article, the complex rheological properties of solutions of a P(VDF-co-HFP) copolymer in a ketone solvent (2-heptanone) in the gel state was investigated. The gels stiffen as they are submitted to LAOS strain. Systems with concentrations between 6 and 10 wt% of copolymer were studied. The apparent strain-hardening is due to the strong nonlinearity of the response, as shown by the shape of stress-strain cycles plotted in the form of Lissajou cycles. This pronounced strain-hardening nonlinearity starts to appear around 20% of deformation amplitude. The degree of strain hardening is roughly independent on concentration.

Abrupt elastic breakdown occurs at strain amplitudes between about 15% and 50% strain amplitude, depending on the gel stiffness. This value should not be considered to be an intrinsic property of the material, as it may correspond to internal fracture or slippage at the walls, and thus depend on experimental conditions. When the high strain amplitude is removed, the solution turns back to a gel with a fast kinetics.

Based on the combined observations presented in this article, the following mechanisms may be tentatively proposed:

MEK and heptanone are not very good solvents for the P(VDF-co-HFP) copolymer. This is particularly true for heptanone. The Flory interaction parameter  $\chi$  is close to the critical value 0.5. It follows that phase separation may be induced by decreasing temperature from above down to room temperature. The solution then separates into two phases, one polymer-rich and one solvent-rich phase. The composition of the phases depend on temperature and the polymer-solvent interaction parameter, while the fraction of each phase in each system depends on the initial copolymer concentration.

SAXS results indicate that identical structures at the scale of a few nanometers are formed by the copolymer, independent of the initial copolymer concentration. These local structures most probably nucleate at the early stage of phase separation.

The elastic response in the linear regime is controlled by the polymer-rich phase (which may be entangled and/or partly crystallized, with crystallites possibly acting as effective crosslinks), which would form a continuous network in the system. The overall modulus value should depend both on the intrinsic modulus of the entangled and/or physically crosslinked polymer-rich phase and on the overall fraction of this phase, that is, on the copolymer concentration.

The response in the nonlinear regime, namely strain-hardening, depends on the intrinsic hyperelastic behavior of the polymer-rich phase. The remarkably strong strain hardening which is observed indicates that this phase should have a high density of effective crosslinks and/or entanglements. To make this statement compatible with a comparatively very low value of the overall linear modulus, the polymer-rich phase should occupy a relatively small fraction of the overall gel system. The strain-hardening behavior does not depend on the overall system concentration, as it is determined by the intrinsic properties of the polymer-rich phase.

After elastic breakdown, the systems recover their initial elastic behavior and the memory of the previous fracture is apparently erased, as judged from the rheological behavior. This illustrates the self-healing ability of the material. This was evidenced in two ways. When the strain amplitude is decreased back to the linear regime progressively, the elastic modulus increases progressively back to the initial value. When the large amplitude strain is stopped and the system maintained at rest, the material recovers its elasticity in a quite short time scale, much shorter than when gelation is induced by cooling down from the liquid state above room temperature.

## ACKNOWLEDGMENTS

We thank Solvay Specialty Polymers for providing the copolymer. We thank Olivier Taché (SWAXS laboratory,

IRAMIS, Saclay, France) for his help with SAXS experiments and Julien Laurens and Guillaume Ovarlez (LoF, Bordeaux, France)) for their help with LAOS experiments.

## DATA AVAILABILITY STATEMENT

Original data may be made available upon request to the corresponding author.

## ORCID

Paul Sotta  <https://orcid.org/0000-0002-4378-0858>

## REFERENCES

- [1] B. Ameduri, *Chem. Rev.* **2009**, 109, 6632.
- [2] B. Ameduri, H. Sawada, *Fluorinated Polymers: From Fundamental to Practical Synthesis*. Volume 2: Applications, RSC, Oxford **2016**.
- [3] B. Ameduri, S. Fomin, *Fascinating Fluoropolymers and Their Applications*, 1st ed., Elsevier, Progress in Fluorine Science Series **2020**.
- [4] R. G. Kepler, R. A. Anderson, *J. Appl. Phys.* **1978**, 49, 4490.
- [5] V. Tomer, E. Manias, C. A. Randall, *J. Appl. Phys.* **2011**, 110, 044107.
- [6] M.-P. Gelin, B. Ameduri, *J. Fluorine Chem.* **2005**, 126, 577.
- [7] R. Hasegawa, Y. Takahashi, Y. Chatani, H. Tadokoro, *Polym. J.* **1972**, 3, 600.
- [8] M. Benz, W. B. Euler, *J. Appl. Polym. Sci.* **2003**, 896, 1093.
- [9] P. Martins, A. C. Lopes, S. Lanceros-Mendez, *Prog. Polym. Sci.* **2014**, 39, 683.
- [10] F. Lederle, C. Härter, S. Beuermann, *J. Fluorine Chem.* **2020**, 234, 109522.
- [11] M. Tazaki, R. Wada, M. Okabe, T. Homma, *J. Appl. Polym. Sci.* **1997**, 65, 1517.
- [12] M. Okabe, R. Wada, M. Tazaki, T. Homma, *Polym. J.* **2003**, 35, 798.
- [13] S. Mal, P. Maiti, A. K. Nandi, *Macromolecules* **1995**, 28, 2371.
- [14] S. Mal, A. K. Nandi, *Langmuir* **1998**, 14, 2238.
- [15] S. Mal, A. K. Nandi, *Polymer* **1998**, 39, 6301.
- [16] A. K. Dikshit, A. K. Nandi, *Macromolecules* **1998**, 31, 8886.
- [17] D. Dasgupta, S. Manna, A. Garai, A. Dawn, C. Rochas, J. M. Guenet, A. K. Nandi, *Macromolecules* **2008**, 41, 779.
- [18] K. Kawanishi, M. Komatsu, T. Inoue, *Polymer* **1987**, 26, 980.
- [19] R. C. Domszy, R. Alamo, C. O. Edwards, L. Mandelkern, *Macromolecules* **1986**, 19, 310.
- [20] D. R. Paul, *J. Appl. Polym. Sci.* **1967**, 11, 439.
- [21] M. Komatsu, T. Inoue, K. Miyasaka, *J. Polym. Sci., Part B: Polym. Phys.* **1986**, 24, 303.
- [22] J. E. Eldridge, J. D. Ferry, *J. Phys. Chem.* **1954**, 58, 992.
- [23] A. Labuzinska, A. Ziabicki, *Kolloid Zeitschrift und Zeitschrift für Polymere* **1971**, 243, 21.
- [24] T. Kanaya, H. Takeshita, Y. Nishikoji, M. Ohkura, K. Nishida, K. Kaji, *Supramol. Sci.* **1998**, 5, 215.
- [25] J. W. Cho, H. Y. Song, S. Y. Kim, *Polymer* **1993**, 34, 1024.
- [26] S. Mortimer, A. J. Ryan, J. L. Stanford, *Macromolecules* **2001**, 34, 2973.
- [27] H. H. Winter, F. Chambon, *J. Rheol.* **1986**, 30, 367.
- [28] J. W. Cho, G. W. Lee, *J. Polym. Sci. Part B: Polym. Phys.* **1996**, 34, 1605.
- [29] B. S. Kim, S. T. Baek, K. W. Song, I. H. Park, J. O. Lee, N. Nemoto, *J. Macromol. Sci. Phys.* **2004**, B43, 741.
- [30] H. Shimizu, Y. Arioka, M. Ogawa, R. Wada, M. Okabe, *Polym. J.* **2011**, 43, 540.
- [31] A. Takahashi, T. Nakamura, I. Kagawa, *Polym. J.* **1972**, 3, 207.
- [32] M. Ohkura, T. Kanaya, K. Kaji, *Polymer* **1992**, 33, 5044.
- [33] P. D. Hong, C. Chou, *Macromolecules* **2000**, 33, 9673.
- [34] P. D. Hong, C. Chou, *Polymer* **2000**, 41, 8311.
- [35] P. J. P. Yadav, G. Ghosh, B. Maiti, V. K. Aswal, P. S. Goyal, P. Maiti, *J. Phys. Chem. B* **2008**, 112, 4594.
- [36] J. Link, O. Sanseau, M. Tauban, F. Colbeau-Justin, P. Sotta, C. Lorthioir, *Macromol. Symp.* **2019**, 385, UNSP 1800162.
- [37] J. S. Higgins, H. C. Benoît, *Polymer and Neutron Scattering*, Clarendon Press, Oxford **1994**.
- [38] A. A. Lefebvre, J. H. Lee, N. P. Balsara, C. Vaidyanathan, *J. Chem. Phys.* **2002**, 117, 9063.
- [39] A. A. Lefebvre, J. H. Lee, N. P. Balsara, B. Hammouda, *J. Chem. Phys.* **2002**, 116, 4777.
- [40] A. A. Lefebvre, J. H. Lee, H. S. Jeon, N. P. Balsara, B. Hammouda, *J. Chem. Phys.* **1999**, 111, 6082.
- [41] H. Tanaka, *J. Phys.: Condens. Matter* **2000**, 12, R207.
- [42] A. Bottino, G. Capannelli, S. Munari, A. Turturro, *J. Polym. Sci. Part B: Polym. Phys.* **1988**, 26, 785.
- [43] C. M. Hansen, *J. Paint Technol.* **1970**, 42, 660.
- [44] J. Brandrup, E. H. Immergut, E. A. Grulke, *Polymer Handbook*, John Wiley & Sons, New York **1999**.
- [45] D. W. van Krevelen, K. te Nijenhuis, *Properties of Polymers: Their Correlation with Chemical Structure; Their Numerical Estimation and Prediction from Additive Group Contributions*, Elsevier, Amsterdam **2009**.
- [46] N. Orakdogan, B. Erman, O. Okay, *Macromolecules* **2010**, 43, 1530.
- [47] R. D. Groot, A. Bot, W. G. M. Agterof, *J. Chem. Phys.* **1996**, 104, 9202.
- [48] Y. Rotbaum, G. Parvari, Y. Eichen, D. Rittel, *Macromolecules* **2017**, 50, 4817.
- [49] K. S. Cho, K. Hyun, K. H. Ahn, S. J. Lee, *J. Rheol.* **2005**, 3, 747.
- [50] A. Papon, S. Merabia, L. Guy, F. Lequeux, H. Montes, P. Sotta, D. R. Long, *Macromolecules* **2012**, 45, 2891.
- [51] P. J. Blatz, S. C. Sharda, N. W. Tschoegl, *Trans. Soc. Rheol.* **1974**, 18, 145.
- [52] J. Zhang, C. R. Daubert, E. A. Foegeding, *J. Food Eng.* **2007**, 80, 157.
- [53] M. Doi, N. Y. Kuzuu, *J. Polym. Sci., Polym. Phys. Ed.* **1980**, 18, 409.

**How to cite this article:** J. Link, M. Tauban, R. Pieri, O. Sanseau, P. Sotta, *J. Polym. Sci.* **2022**, 1. <https://doi.org/10.1002/pol.20220156>